

Estimation of Atomic Oxygen Concentration by Semi-empirical Collisional-Radiative Model in High Enthalpy Flow

Makoto Matsui¹, Hiroki Takayanagi², Yasuhisa Oda³, Kimya Komurasaki⁴,
and Yoshihiro Arakawa⁵

^{1,3,4}Department of Advanced Energy, The University of Tokyo,
Kashiwanoha 5-1-5, Kashiwa, Chiba 277-0882, Japan

^{2,5}Department of Aeronautics and Astronautics, The University of Tokyo,
Hongo 7-3-1, Bunkyo, Tokyo 113-0033, Japan

Keywords: collisional-radiative model, high enthalpy flow, laser absorption spectroscopy

Abstraction

Collisional-radiative model for atomic oxygen was applied to arc-heater plumes to clarify a mechanism of population density. The model with input parameters obtained by laser absorption spectroscopy and a single probe measurement shows consistent results with that of emission spectroscopy. As a result, the population density was found not to obey the Boltzmann distribution. The number density of ground level was estimated 20% lower than that in Boltzmann distribution.

1. Introduction

In developing thermal protection systems for reentry vehicles, arc-heaters are often used to simulate reentry conditions. However, their exact plume conditions are mostly unknown because they are usually in strong thermo-chemical non-equilibrium.¹⁻³⁾ Although various intrusive and non-intrusive measurements such as probe and spectroscopic methods have been actively applied to the characterization of such high enthalpy plumes, and the electron density, temperature and vibration, and rotational temperatures of atoms and molecules in the plumes are gradually clarified, it is still difficult to measure the chemical compositions by these spectroscopic methods.

In our previous research⁴⁻⁶⁾, number density of meta-stable atomic oxygen in the University of Tokyo arc-heater plume was measured by laser absorption spectroscopy as shown in Fig.1. As a result, the number density was found in the order of 10^{16} m^{-3} . However, number density of total

atomic oxygen, most of which is in ground level, is difficult to be deduced from the meta-stable one because its electronic excitation would not be in thermal equilibrium. Then, in this study, relationship between measured meta-stable oxygen and ground level oxygen was investigated developing a collisional-radiative model.

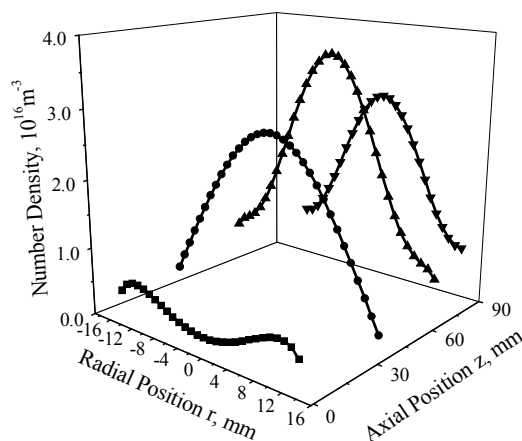


Fig.1 Number density distributions of meta-stable atomic oxygen in the University of Tokyo arc-heater plume

¹⁻³Graduate students, Student Member AIAA

⁴Associate Professor, Senior Member AIAA

⁵Professor, Senior Member AIAA

Copyright © 2004 The American Institute of Aeronautics and Astronautics Inc. All right reserved.

2. Collisional-Radiative Model

Although collisional-radiative models for various gases have been discussed, most of them are developed to estimate electron temperature or electron density combined with emission spectroscopy.⁷⁻¹⁴⁾ Models for number density estimation have not been developed.

In this study, the collisional-radiative model for atomic oxygen developed by Kunc was based.⁷⁻¹⁰⁾ Since this model is aimed for ionizing plasma, only electron-impact excitation and spontaneous emission in low excited levels are considered as transition processes. On the other hand, high enthalpy flows for TPS tests are usually recombining plasma. Then, effects of higher levels and ion are added to the model.

2.1 Levels

Park's model was used.¹⁵⁾ In this model, internal levels are categorized to 19 levels as tabulated in Table 1. Here, i is the level number, g is the statistical weight and E is the excitation energy, respectively. Then, according to the Kunc' model, these 19 levels are divided into three zones: Boltzmann, Active and Saha zones.

Boltzmann zone

The levels with $i = 1, 2$ and 3 almost always have Boltzmann distribution⁹⁾:

$$\frac{n_i}{n_1} = \frac{g_i}{g_1} \exp\left(-\frac{E_i}{k_B T_e}\right) \quad (1)$$

Here, n is the number density, k_B is the Boltzmann constant and T_e is the electron temperature, respectively. Then, n_2 and n_3 are represented by the function of n_1 and T_e .

Active zone

Since Griem boundary p_G and Byron boundary p_B defined below are 2.8 and 2.6 at T_e of 8000K and n_e of 10^{19}m^{-3} , respectively, levels whose principal quantum number p is 3 are categorized to Active zone. Rate equations for these levels with $i = 4 \sim 7$ are considered.^{10, 16-20)}

$$p_G = 95n_e^{-17/2} \quad (2)$$

$$p_B = \sqrt{\frac{R}{3k_B T_e}} \quad (3)$$

Here, n_e is electron density and R is Rydberg constant.

Saha zone

Since principal quantum number of levels with $p > 8$ is enough larger than p_G and p_B , these levels are almost in Saha equilibrium. Then, n_i is related to number density of atomic oxygen ion n_{O^+} and n_e as,

$$n_i = Z_i n_{O^+} n_e$$

$$Z_i = \frac{g_i}{2g_+} \left(\frac{h^2}{2\pi k_B T_e} \right)^{3/2} \exp\left(-\frac{\chi_i}{k_B T_e}\right). \quad (4)$$

Here, Z is Saha-Boltzmann constant and χ is the ionization energy, respectively. The Grotrian diagram is shown in Fig.2.

2.2 Rate equations

Assuming the quasi steady state condition, rate equations for $i = 4 \sim 7$ are expressed as,

$$\sum_{q < p} C_{qp} n_e n_q - \left[\sum_{q < p} F_{pq} + \sum_{q > p} C_{pq} + S_p \right] n_e + \sum_{q < p} A_{pq} \Big] n_i + \sum_{q > p} \left[F_{qp} n_e + A_{qp} \right] n_i + \left[\alpha_p n_e + \beta_p \right] n_{O^+} n_e. \quad (5)$$

Here, $C, F, S, A, \alpha, \beta$ are the rate coefficients of electron-impact excitation, electron-impact de-excitation, electron-impact ionization, spontaneous emission, three-body recombination and radiative recombination, respectively.

Table 1 level

No	Configuration	g	E, eV
1	2p ⁴ 3P	9	0.00967
2	2p ⁴ 1D	5	1.967315
3	2p ⁴ 1S	1	4.189532
4	3s ⁵ S	5	9.145757
5	3s ³ S	3	9.521044
6	3p ⁵ P	15	10.74026
7	3p ³ P	9	10.98847
8	4s ⁵ S, 4s ³ S	8	11.87195
9	3d ⁵ D, 3d ³ D	40	12.08123
10	4p ⁵ P, 4p ³ P	24	12.31283
11	5s ⁵ S, 5s ³ S	8	12.6741
12	4d ⁵ D, 4f ⁵ F, 4d ³ D, 4f ³ F	96	12.75519
13	5p ⁵ P, 5p ³ P	24	12.87768
14	5d ⁵ D, 5f ⁵ F, 5g ⁵ G, 5d ³ D, 5f ³ F, 5g ³ F	168	13.06675
15	n=6	288	13.2211
16	n=7	392	13.33814
17	n=8	512	13.40435
18	n=9	648	13.4491
19	n=10	800	13.48084
Ion	2p ³ 4S	4	13.61806

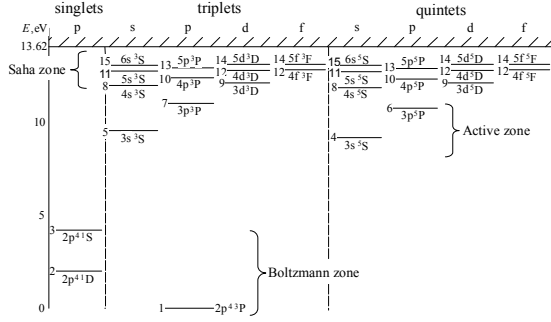


Fig.2 Grotrian diagram of OI

2.3 Rate coefficients

Electron-impact excitation/de-excitation

Rate coefficients of electron-impact excitation C are referred to Park's data.¹⁵⁾ Reverse rate F were estimated by the principle of detailed balance expressed as,

$$F_{p,q} = C_{q,p} \frac{g_q}{g_p} \exp\left(-\frac{E_{pq}}{k_B T_e}\right). \quad (6)$$

Spontaneous emission

All data of A is referred to NIST.²¹⁾ Although atomic oxygen has 910 emission lines, for simplicity, those from levels with $p > 5$ are neglected. Moreover the rest 60 lines are reduced to 14 lines considering the statistical weight as tabulated in Table 2.

Table2 Einstein coefficient, $10^8 s^{-1}$

A_{51}	2.65	A_{105}	0.008	A_{87}	0.093
A_{81}	0.733	A_{86}	0.099	A_{117}	0.029
A_{64}	0.369	A_{116}	0.030	A_{97}	0.179
A_{104}	0.005	A_{96}	0.247	A_{127}	0.020
A_{75}	0.322	A_{126}	0.042		

Electron-impact ionization

Rate coefficient of electron-impact ionization from ground level S_1 is referred to Lee²²⁾, which is a fit to the rate coefficient given by Eliasson and Kogelshatz.²³⁾

$$S_1 = 9 \times 10^{-9} T_e^{0.7} \exp(-\chi_1 / k_B T_e) \quad (7)$$

The coefficients from the other levels are estimated by the Thomson formula²⁴⁾ and S_1 .

$$S_i = K \pi e^4 \frac{8^{1/8}}{(\pi m_e)^{1/2} (k_B T_e)^{3/2}} \frac{\chi_i}{k_B T_e} \left(1 + \frac{\chi_i}{k_B T_e}\right) \exp\left(-\frac{\chi_i}{k_B T_e}\right) \quad (8)$$

Here, m_e is the mass of electron, e is the electron charge and K is the fitting parameter, respectively.

Three-body recombination

Rate coefficient of three-body recombination

α is estimated by the principle of detailed balance with S and Z .

$$\alpha_i = Z_i S_i. \quad (9)$$

Radiative recombination

Rate coefficient of radiative recombination to the ground level β_1 for $T_e = 100K, 1000K, 10000K$ is taken from Nahar. Dependency on temperature of β_1 is estimated by linear interpolation.²⁵⁾ For the other levels, β_i is estimated by the scaling rule of Fujimoto.¹⁷⁾

$$\beta_i = \frac{2^6}{3\sqrt{3}} \frac{\sqrt{\pi} e^4}{m_e^2 c^3} \frac{1}{p^3} \left(\frac{R}{k_B T}\right)^{3/2} \exp\left(\frac{\chi_i}{k_B T_e}\right) \int_{\frac{\chi_i}{k_B T_e}}^{\infty} \frac{e^{-t}}{t} dt \quad (10)$$

2.4 Calculation process

For 22 parameters ($n_i (i=1\sim 19), n_e, n_+$ and T_e), there are 8 unknown parameters ($n_i (i=1,4\sim 7), n_e, n_+$ and T_e) and 18 equations (Eqs.(4,5,9)). Then, four parameters are necessary to solve the rate equations.

In this study, n_4, n_e, n_{O+} and T_e are chosen as input parameters. Here, n_4 is obtained from laser absorption spectroscopy, n_e and T_e are obtained from a single probe method or emission spectroscopy and n_{O+} is a tuning parameter.

3. Input Conditions

Details of the arc-heater and laser absorption spectroscopy measurement are described in the reference [4-6].

In addition, emission spectroscopy and a single probe measurement have been applied to obtain electron density and temperature. Here, electron temperature was estimated by OI and ArI emission lines, respectively. Observed emission lines and their transition data are shown in Fig.3 and Table 3. Since observed ArI lines are emissions from higher levels than the Byron boundary, these levels are considered close to LTE. Then, estimated T_e by ArI lines was adopted as an input parameter.

Since n_{O+} is not equal to n_e for the presence of argon ion and molecular oxygen ion, n_{O+} is also necessary to be determined. Here, the ration of n_{O+} to n_e is set to be 0.1, which corresponds to thermo-chemical equilibrium. Then, the ratio is changed from 1 to 0.001.

All experimental results are summarized in Table 4.

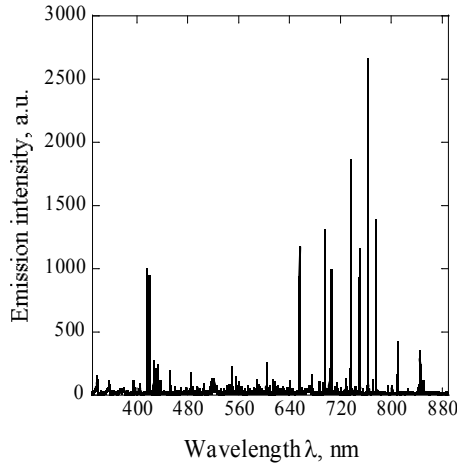


Fig.3 Emission lines

Table 3 Observed emission lines

Species	λ [nm]	i	j
OI	615.82	$3p^5P$	$4d^5D$
OI	645.60	$3p^5P$	$5s^5S$
OI	777.19	$3s^5S$	$3p^5P$
OI	844.64	$3s^3S$	$3p^3P$
ArI	588.86	$4p^2[5/2]$	$7s^2[3/2]$
ArI	591.21	$4p^2[1/2]$	$4d^2[3/2]$
ArI	603.21	$4p^2[5/2]$	$5d^2[7/2]$
ArI	641.63	$4p^2[1/2]$	$6s^2[3/2]$
ArI	794.82	$4s^2[1/2]$	$4p^2[3/2]$
ArI	800.62	$4s^2[3/2]$	$4p^2[3/2]$
ArI	801.48	$4s^2[3/2]$	$4p^2[5/2]$
ArI	810.37	$4s^2[3/2]$	$4p^2[3/2]$
ArI	811.53	$4s^2[3/2]$	$4p^2[5/2]$
ArI	840.82	$4p^2[1/2]$	$4p^2[3/2]$
ArI	842.46	$4p^2[3/2]$	$4p^2[5/2]$

Table 3 Input parameters

n_4, m^{-3} (LAS)	n_e, m^{-3} (Probe)	T_e, K (ES, ArI)	T_e, K (ES, OI)	T_{tr}, K (LAS)
1×10^{16}	1×10^{19}	8000	3300	2200K

4. Results and Discussion

4.1 Results

Figure 4 shows calculated results with various n_{O^+}/n_e . As shown in this figure, number density in lower levels is almost independent of n_{O^+}/n_e . This means that three-body and radiative recombination doesn't contribute to increase of number density in those levels.

On the other hand, number density in higher levels has strong dependence on n_{O^+}/n_e . Table 4

shows T_e estimated by Boltzmann plot of calculated $n_6 \sim n_{12}$, whose levels were detected in the emission spectroscopy. The result shows the model is consistent with the result of emission spectroscopy.

Table 5 shows calculated n_1 and that estimated from Boltzmann plot. As seen in this table, estimated n_1 by CR model is 20% less than that estimated by Boltzmann plot.

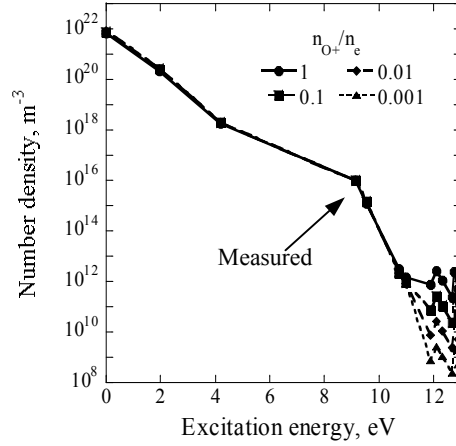


Fig.4 Calculated number density for various n_{O^+}/n_e

Table 4 Estimated T_e

n_{O^+}/n_e	T_e, K
1	1183
0.1	5562
0.01	3467
0.001	2504
ES, OI	3300

Table 5 Estimated n_1

CR model	Boltzmann plot
$8.00 \times 10^{22}, m^{-3}$	$1.03 \times 10^{23}, m^{-3}$

4.2 Discussion

To validate this model, sensitivity analysis was applied.

n_e dependency

Dependency of n_e on n_i is shown in Fig.5. Number density in lower levels (n_1, n_5) is almost constant with $n_e < 10^{21} m^{-3}$ and then, rapidly decreases. This sudden decrease is due to the ionization. On the other hand, number density in higher levels (n_6, n_7) increases with n_e . Therefore, in arc-heater plumes ($10^{17} m^{-3} < n_e < 10^{20} m^{-3}$), n_e is not so important for n_1 estimation.

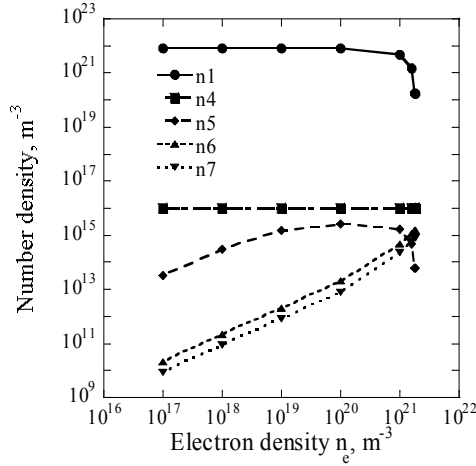


Fig.5 n_e dependency
($n_4=10^{16} \text{ m}^{-3}$, $T_e=8000\text{K}$, $n_{\text{O}^+}/n_e=0.01$)

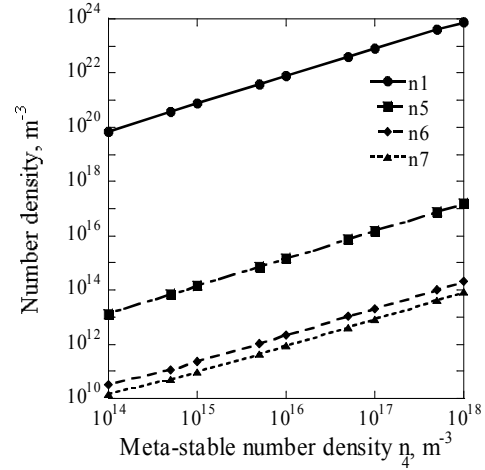


Fig.7 n_4 dependency
($n_e=10^{19} \text{ m}^{-3}$, $T_e=8000\text{K}$, $n_{\text{O}^+}/n_e=0.01$)

T_e dependency

Dependency of T_e on n_i is shown in Fig.6. Although number density in higher levels (n_5 , n_6 , n_7) is almost constant, n_1 increases with T_e . Therefore, T_e is most carefully measured for n_1 estimation.

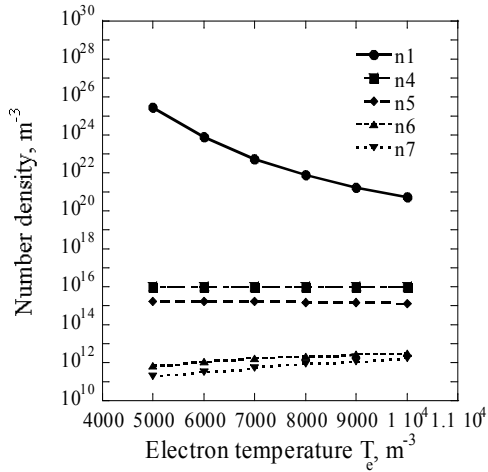


Fig.6 T_e dependency
($n_e=10^{19} \text{ m}^{-3}$, $n_4=10^{16} \text{ m}^{-3}$, $n_{\text{O}^+}/n_e=0.01$)

n_4 dependency

Dependency of n_4 on n_i is shown in Fig.7. Number density in all levels almost linearly increases with n_4 .

5. Conclusion

- Collisional radiative model for atomic oxygen was developed.
- Calculated number density of higher levels is consistent with the result of emission spectroscopy.
- OI excited levels with $p=3$ are in non-equilibrium and cannot be used for the determination of electron temperature.
- Number density of ground level was estimated to 20% lower than that in Boltzmann distribution.

Reference

- 1) Salinas, I. T., Park, C., Strawa, A.W., Gopaul N. and Taunk, A.W.: Spectral Measurements in the Arc Column of an Arc-Jet Wind Tunnel, AIAA Paper 94-2595, 1994
- 2) Winter, M. W. and Auweter-Kurtz, M.: Boundary layer investigation in front of a blunt body in a subsonic air plasma flow by emission spectroscopic means, AIAA paper 98-2460, 1998.
- 3) Laux, T., Feigl, M., Auweter-Kurtz, M. and Stockle, T.: Estimation of the Surface Catalycity of PVD-Coatings by Simultaneous Heat Flux and LIF Measurements in High Enthalpy Air Flows, AIAA Paper 00-2364, 2000
- 4) Matsui, M. Komurasaki, K. and Arakawa, Y.: Laser Diagnostics of Atomic Oxygen in Arc-heater Plumes, AIAA Paper 02-0793, 2002
- 5) Matsui, M. Komurasaki, K. and Arakawa, Y.:

- Characterization of Arc-jet Type Arc-heater Plumes, AIAA Paper 02-2242, 2002
- 6) Matsui, M., Satoshi, O., Komurasaki, K., Arakawa, Y.: Arc-heater as an Atomic Oxygen Generator, AIAA Paper 03-3903, 2003
 - 7) Braun, C. G. and Kunc J. A.: Collisional-radiative coefficients from a three-level atomic mode in nonequilibrium argon plasmas, physics of fluid, vol.30, No.2, 499-509, 1987
 - 8) Kunc, J. A. and Soon, W. H.: Collisional-radiative nonequilibrium in partially ionized atomic nitrogen, physical review A, vol.40, No.10, 5822-5843, 1989
 - 9) Kunc, J. A. and Soon, W. H.: Thermal nonequilibrium in partially ionized atomic oxygen, Physical Review A, vol. 41, 825-843, 1990
 - 10) Gordillo-Vazquez, F. J. and Kunc, J. A.: Diagnostics of plasmas with substantial concentrations of atomic oxygen, Physical Review E, vol.51, No.6, 6010-6015, 1995
 - 11) Vlcek, J. and Pelikan, V.: A collisional-radiative model applicable to argon discharges over a wide range of conditions. I : Formulation and basic data, journal of physics D, vol.24, 309-317, 1991
 - 12) Vlcek, J. and Pelikan, V.: A collisional-radiative model applicable to argon discharges over a wide range of conditions. IV : Application to inductively coupled plasmas, journal of physics D, vol.24, 309-317, 1991
 - 13) Colonna, G., Pietanza, L.D. and Capitelli, M.: A collisional radiative model for Xe electrical thrusters, AIAA Paper 00-2349, 2000
 - 14) K. Kano and H. Akatsuka: Spectroscopic Measurement of Electron Temperature and Density in Argon Plasmas Based on Collisional-Radiative Model (Invited Paper); Chapter 3, Advances in Plasma Physics research, 3, 55-85, NOVA Sciece and Publishers, Inc., New York 2002
 - 15) Park, C.: Nonequilibrium hypersonic aerothermodynamics, John Wiley & Sons Inc, 1990
 - 16) Fujimoto, T.: Kinetics of ionization recombination of a plasma and population density of excited ions. I . Equilibrium plasma, Journal of the physical society of Japan. Vol.47, No.1, 265-272, 1979
 - 17) Fujimoto, T.: Kinetics of ionization recombination of a plasma and population density of excited ions. II . Ionizing plasma, Journal of the physical society of Japan. Vol.47, No.1, 273-281, 1979
 - 18) Fujimoto, T.: Kinetics of ionization recombination of a plasma and population density of excited ions. III . Recombining plasma, Journal of the physical society of Japan. Vol.49, No.4, 1561-1568, 1980
 - 19) Fujimoto, T.: Kinetics of ionization recombination of a plasma and population density of excited ions. IV V . Recombining plasma: low -temperature case, Journal of the physical society of Japan. Vol.49, No.4, 1569-1576, 1980
 - 20) Fujimoto, T.: Kinetics of ionization recombination of a plasma and population density of excited ions. V . Ionization recombination and equilibrium plasma, Journal of the physical society of Japan. Vol.54, No.8, 2905-2914, 1985
 - 21) http://physics.nist.gov/cgi-bin/AtData/main_sd
 - 22) Lee, C. Lieberman, M. A. and Hess, D. W.: Global model of plasma chemistry in a high density oxygen discharge, Journal of the Electrochemical Society, vol.141, 1546-1555, 1994
 - 23) Eliasson, B. and Kogelshatz, U.: Basic data for modeling of electrical discharges in gases: Oxygen, Report KLR-11C, Brouwn Boveri Konzernforschung, CH5405, 1986
 - 24) Kimura, A., Minomo M. and Nishida, M.: Population density measurements in a partially ionized nonequilibrium freejet expansion flow, International symposium on rarefied gas dynamics, 969-976, 1978
 - 25) S. N. Nahar: Electron-ion recombination rate coefficients, photoionization cross sections, and ionization fractions for astrophysically abundant elements. II. Oxygen ion, Astrophysical journal supplement series, 120, 131-145, 1999